



Evaluating the Precision of Wheat Actual Evapotranspiration with the Vegetation Index Method in Comparison to the Metric Model

Omar Alsenjar¹ · Mahmut Cetin¹

¹Department of Agricultural Structures and Irrigation, Cukurova University, Adana, Türkiye

oalsenjar@cu.edu.tr/ omarsenjar@yahoo.com

Abstract. Accurate estimation of actual evapotranspiration (ET_a) is crucial for sustainable water resource management, particularly in large-scale irrigation districts. This study presents a comparative evaluation of the METRIC and Kc-NDVI models for estimating ET_a of wheat during two consecutive hydrological years (2020 and 2021) in the Akarsu Irrigation District (9,495 ha), located in the Lower Seyhan Plain, southern Türkiye. The METRIC model integrates multiple remote sensing and meteorological inputs, whereas the Kc-NDVI method relies on fewer data sources, making it suitable for data-scarce regions. Fourteen clear-sky Landsat 7 and 8 images, together with climate data from two local meteorological stations, were used to estimate seasonal ET_a of wheat. Results showed that the Kc-NDVI method consistently underestimated ET_a for wheat compared with the METRIC model, particularly at the beginning and end of the winter growing season. The Mean Bias Errors (MBE) were 0.61 mm/day and 0.78 mm/day, while the Root Mean Square Errors (RMSE) were 0.86 mm/day and 0.97 mm/day for 2020 and 2021, respectively. Despite its simplified input requirements, the Kc-NDVI method demonstrated satisfactory performance during the mid-season period. These findings highlight the potential of the Kc-NDVI approach as a cost-effective and operationally feasible alternative for field-scale ET_a estimation and irrigation management in data-limited environments.

Keywords: Actual evapotranspiration, remote sensing, NDVI, Crop coefficient, Akarsu Irrigation District

1 Introduction

Wheat is a strategic crop because it meets the nutritional needs of humans and animals and remains essential to livelihoods. Consequently, accurately estimating actual evapotranspiration (ETa) for wheat and other crops is crucial for large-scale irrigation management. In contrast to direct ETa estimation techniques, which provide only point or near-point observations (such as weighing lysimeters, Bowen ratio energy balance systems (BREBS), eddy covariance (EC), scintillometers, or soil-water balance methods (Zhang et al., 2011)), remote sensing (RS) approaches enable ETa estimation over extensive areas using multiple models (Su, 2002; Allen et al., 2007b; Alsenjar et al., 2023b; Çetin et al., 2023a, 2023b).

Among remote sensing (RS)-based surface energy balance methods, Mapping Evapotranspiration at High Resolution with Internalised Calibration (METRIC) (Allen et al., 2007a, 2007b) has been widely adopted for quantifying evapotranspiration (ETa) across spatial scales and vegetation types. In our study area, the Akarsu Irrigation District (AID) in the Lower Seyhan Plain in southern Turkey, METRIC has been used to map ETa for crops such as wheat, potatoes, and lettuce (Alsenjar et al., 2023b; Çetin et al., 2023a, 2023b). METRIC requires numerous inputs, including shortwave and thermal infrared imagery, a digital elevation model (DEM), land surface temperature (Ts), the normalised difference vegetation index (NDVI), albedo, emissivity, and meteorological variables, as well as substantial pre-processing, which is best handled by experienced remote sensing (RS) analysts (Foolad et al., 2018). To reduce complexity, a vegetation-index approach has been proposed to produce ETa maps with fewer inputs.

The vegetation-index method (Kamble et al., 2013; El-Shirbeny et al., 2015; Reyes-González et al., 2018) leverages the relationship between the crop coefficient (Kc) and NDVI to derive a revised crop coefficient of Kc-NDVI. ETa is then computed as Kc-NDVI multiplied by reference evapotranspiration (ETo). In this regard, the Kc-NDVI approach offers a more straightforward, faster method for generating ETa maps from satellite-derived vegetation indices, using limited ancillary data. As NDVI captures canopy density and reflects the actual condition of the crop at the time of satellite overpass, many studies report a roughly linear relationship between Kc and NDVI under well-watered conditions (Rafn et al., 2009; Kamble et al., 2013; El-Shirbeny et al., 2015; Reyes-González et al., 2018).

In this study, wheat actual evapotranspiration (ETa) was estimated using two approaches: (i) the physics-based METRIC model, which relies on detailed energy balance equations and extensive input data, and (ii) the Kc-NDVI method, which requires fewer input variables. The novelty of this research lies in the direct, side-by-side comparison of wheat ETa estimates derived from the Kc-NDVI and METRIC models to assess the performance of the simplified Kc-NDVI approach in the Akarsu Irrigation District (AID) during the 2020 and 2021 hydrological years. To the best of our knowledge, no previous study has jointly applied and compared these two remote-sensing-based ETa estimation techniques for wheat in this region of Türkiye. The specific objectives were to (a) compare METRIC-based and Kc-NDVI-based ETa estimates and (b) quantify their statistical relationship. More broadly, this study provides the first demonstration of the Kc-NDVI method for generating spatially distributed ETa maps

as a simple, rapid alternative to more data-intensive remote-sensing techniques in a large-scale irrigation district of the Eastern Mediterranean region. Furthermore, the approach holds potential for generalization to daily ET_a estimation across diverse agro-climatic conditions worldwide.

2 Materials and Methods

The methodology framework followed in this study is presented in Figure 1. Figure 1 summarizes the details of the data and the used methods for ET_a estimation with METRIC and K_c -NDVI. Inputs include Landsat red/NIR bands, as well as local climatic data. Derived variables are NDVI, crop coefficient (K_c), net radiation (R_n), soil heat flux (G), and sensible heat flux (H). Outputs are ET_a maps from both methods, which are subsequently compared.

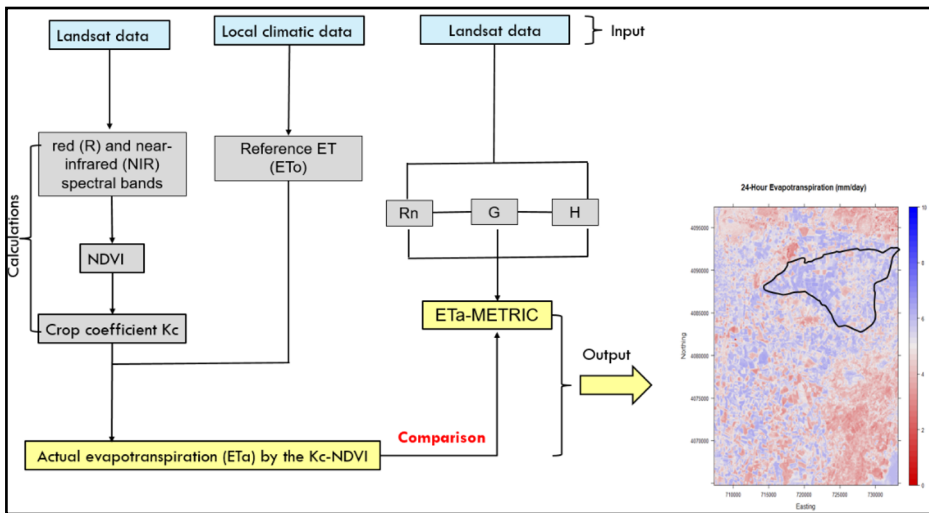


Fig. 1. Workflow for estimating actual evapotranspiration (ET_a) using remote sensing and meteorological data. The process integrates input datasets (Landsat imagery and weather station data), intermediate computations (NDVI, crop coefficient (K_c), net radiation (R_n), soil heat flux (G), and sensible heat flux (H)), and final outputs representing ET_a estimates derived from the K_c -NDVI and METRIC models.

2.1 Study site and in-situ climatic data

The study was conducted in the Akarsu Irrigation District (AID; 9,495 ha), located within the intensively cultivated Lower Seyhan Plain (LSP) of southern Türkiye (Figure

2). The region has a typical Mediterranean climate, characterized by hot, dry summers and mild, wet winters, which are highly suitable for agricultural production. The mean annual air temperature is 18.9 °C, with average minimum and maximum temperatures of 9.0 °C and 31.0 °C, respectively. The mean annual precipitation across the basin is approximately 650 mm (Çetin, 2020; Çetin et al., 2020). The hydrological year (HY) extends from 1 October to 30 September (12 months; 365 days). The Akarsu Irrigation District (AID) is located within the intensively cultivated Lower Seyhan Plain (LSP) and represents a sub-basin managed under regional irrigation governance. From 1994 to 2018, irrigation operations in the AID were managed by the Akarsu Irrigation Association. On 25 January 2019, this association was dissolved, and all irrigation associations operating on the left bank of the Lower Seyhan Plain were unified under a single administrative body, the Seyhan Left Bank Irrigation Association. The AID currently functions as a sub-basin within the association's operation and maintenance jurisdiction (İbrikçi et al., 2015; Alsenjar et al., 2023b). Table 1 summarizes the dominant winter crops for the 2020 and 2021 hydrological years. As presented in Table 1 and Figure 2, wheat covered 1,187 ha (12.5%) in winter 2020 and 1,548 ha (16.3%) in winter 2021 (Alsenjar et al., 2023a, 2023b). These proportions were obtained from coordinated winter field campaigns conducted in both years and from a supervised classification workflow integrating remote-sensing data with ground-truth observations. Specifically, crop types were classified using an artificial neural network (ANN) classifier trained with field-verified reference samples and phenology-based spectral features. The resulting crop maps were further validated through in situ observations to refine class boundaries and reduce both commission and omission errors. Detailed descriptions of the training dataset preparation, feature selection, classifier configuration, and post-classification validation are provided in Alsenjar et al. (2023a, 2023b).

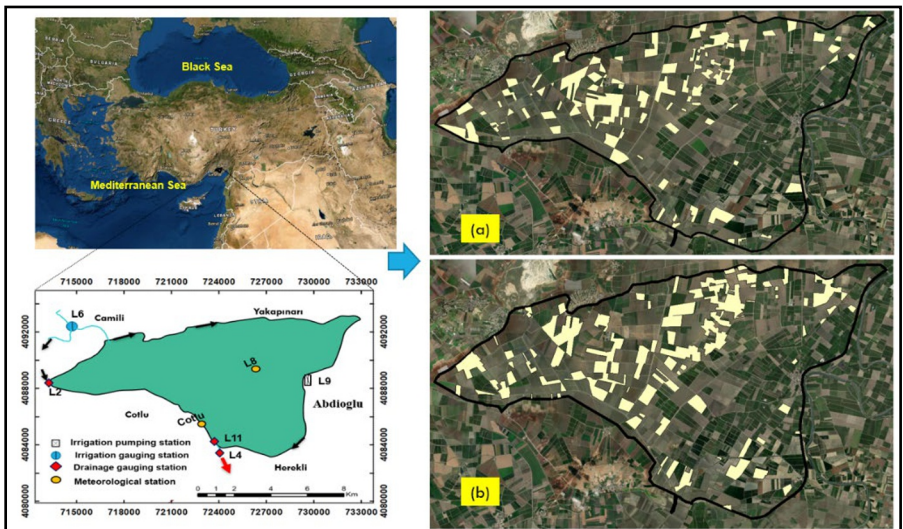


Fig. 2. Location of the Akarsu Irrigation District (AID) within the Lower Seyhan Plain, south-eastern Türkiye. The map indicates meteorological (L8, Çotlu), irrigation (L6, L9), and drainage (L2, L11) gauging stations, as well as the drainage outlet (L4). Panels (a) and (b) show wheat fields mapped for the 2020 and 2021 hydrological years, respectively.

Table 1. Percentage of major crop coverages in the Akarsu Irrigation District (AID) during the 2020 and 2021 growing seasons (Alsenjar et al., 2023a, 2023b).

Crop types	Winter 2020	Winter 2021
Wheat	12.5	16.3
Citrus	39.9	39.4
Other	47.6	44.3

2.2 Landsat Image Data Availability

In this study, 14 clear-sky Landsat scenes (Landsat 7 and Landsat 8; WRS-2 path 175/row 34) were utilized, obtained from the USGS Earth Explorer platform (<http://earthexplorer.usgs.gov>) with a spatial resolution of 30 × 30 m. The image characteristics are summarized in Table 1. Scan Line Corrector (SLC) gaps in Landsat 7 scenes were corrected using Quantum Geographic Information System (QGIS 3.24.3), and cloud masking was performed in the Environment for Visualizing Images (ENVI) software for two affected dates (DOY 28 and DOY 60; see Table 1).

Table 2. Landsat imagery and overpass local times used for actual evapotranspiration (ETA) estimation in the Akarsu Irrigation District (AID).

Water year (HY)	Image	Day of the year (DOY)	Landsat scene-ID	Landsat type	Cloud cover (%)	Acquisition dates	Overpass local time (AM)
2020	1	321	LC81750342019321LGN00	8	4	17.11.2019	11:16:01.7353690
	2	353	LC81750342019353LGN01	8	1	19.12.2019	11:15:58.3225900
	3	28	LE71750342020028NPA00	7	67	28.01.2020	10:55:13.3874493
	4	60	LE71750342020060SG100	7	66	29.02.2020	10:53:33.8472536
	5	68	LC81750342020068LGN00	8	2	08.03.2020	11:15:36.2460760

Water year (HY)	Image	Day of the year (DOY)	Landsat scene-ID	Landsat type	Cloud cover (%)	Acquisition dates	Overpass local time (AM)
	6	108	LE71750342020108SG100	7	6	17.04.2020	10:50:52.5176873
	7	148	LC81750342020148LGN00	8	4	27.05.2020	11:15:08.7684079
	8	316	LE71750342020316NPA00	7	3	11.11.2020	10:37:51.0228172
2021	9	364	LE71750342020364NPA00	7	1	29.12.2020	10:34:21.8153233
	10	22	LC81750342021022LGN00	8	9	22.01.2021	11:15:49.9861710
	11	54	LC81750342021054LGN00	8	7	23.02.2021	11:15:43.2139690
	12	79	LE71750342021078SG100	7	5	19.03.2021	10:28:24.8443048
	13	118	LC81750342021118LGN00	8	8	28.04.2021	11:15:15.8809360
	14	134	LC81750342021134LGN00	8	1	14.05.2021	11:15:15.9098560

2.3 Normalized Difference Vegetation Index (NDVI) Calculation

The NDVI is one of the essential indicators used remotely to assess vegetation health, coverage, and crop growth stages at each satellite image pixel, based on reflected light in the visible and near-infrared bands. The NDVI is computed as the ratio of the measured intensities in the red (R) and near-infrared (NIR) spectral bands (Rouse et al., 1973; Alsenjar et al., 2023b) using the following formula (1):

$$NDVI = \frac{NIR - R}{NIR + R} \quad (1)$$

Where R and NIR denote the red and near-infrared surface reflectance, respectively, NDVI values range from -1 to 1. Before computation, all scenes were quality-filtered to remove clouds, shadows, and snow to prevent spurious values. In general, NDVI values < 0 indicate water or residual shadow, values between ~0 and 0.2 correspond to bare or senescent surfaces, ~0.2–0.5 represent sparse to moderate vegetation, and > 0.5 denote dense green vegetation. Because NDVI tends to saturate under high-biomass conditions, the patterns were cross-verified, where necessary, using complementary vegetation indices such as the Enhanced Vegetation Index (EVI) and red-edge-based metrics.

2.4 Crop Coefficient (K_c) Curves for NDVI-Based Method

For this study, local wheat crop coefficients (K_c) for the various growth stages were obtained from existing literature (TAGEM-DSI, 2017; Alsenjar et al., 2023b; Çetin et al., 2023a). As is well known, K_c values characterise crop conditions across the initial, developmental, mid-season (second and third stages) and late-season phases, as illustrated in Figure 3. These stage-specific K_c values were then used to convert reference evapotranspiration (E_{To}) to crop evapotranspiration (E_{Tc}), thereby ensuring that the water-use estimates accurately reflect the local cultivar, climate and management conditions.

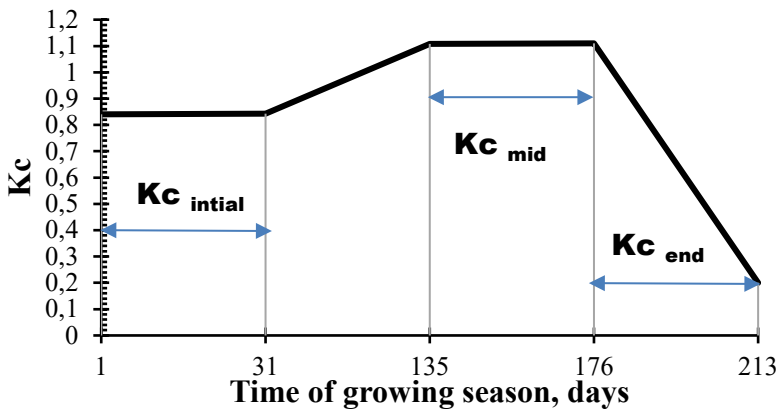


Fig. 3. Schematic representation of the wheat crop coefficient (K_c) curve throughout the growing season, from planting to harvest (adapted from Allen et al., 1998).

2.5 Estimation of E_{Ta} Using the K_c -NDVI Method Based on the Relationship Between K_c and NDVI

To estimate actual evapotranspiration (E_{Ta}) using the K_c -NDVI method, linear regressions were established between the normalized difference vegetation index (NDVI) and crop coefficient (K_c) for each Landsat overpass during the winter seasons of 2020 and 2021 (Kamble et al., 2013; El-Shirbeny et al., 2015; Reyes-González et al., 2018).

These regression relationships were then applied to generate Kc–NDVI maps, representing spatially distributed Kc values. Using ArcGIS 10.4.1, spatially explicit Kc layers were produced and subsequently multiplied by reference evapotranspiration (ET_o) derived from climatic data recorded at two weather stations (see Figure 2), yielding ET_a maps for both growing seasons.

2.6 METRIC Model

We used the METRIC model to calculate the actual evapotranspiration rate (ET_a; referred to hereafter as ET_a-METRIC) at pixel, crop type and whole area scales (see Eq. 2). This involved using Landsat imagery alongside ground-based hourly meteorological data from the L8 and Cotlu stations, acquired at the time of the satellite overpass, in accordance with the methodology outlined by Allen et al. (2007a, 2007b).

$$LE = R_n - G - H \quad (2)$$

Where LE stands for latent heat, R_n is net radiation, H is sensible heat, and G is soil heat flux. All the fluxes are in the unit of watts per square meter (i.e., $W\ m^{-2}$). The standard *METRIC* model was adapted into the R-METRIC model using a water package in the R programming language (Olmedo et al., 2016) and the LandMOD ET mapper in MATLAB (Bhattarai et al., 2017). Reference evapotranspiration (ET_o) in $mm\ day^{-1}$ unit was applied by the *FAO-Penman-Monteith* approach (Allen et al., 1998). Further information on the METRIC model and its equations, particularly the ET_a calculation, can be found in the work of Allen et al. (2007a, 2007b).

2.7 Statistical Analysis between ET_a-Kc-NDVI and ET_a-METRIC

This paper statistically assesses the difference between *ET_a-Kc-NDVI* and *ET_a-METRIC* using a simple linear regression approach ($y = a + bx$), where y is *ET_a* by *Kc-NDVI* and x is *ET_a-METRIC* over the AID at the dates when the satellite images were acquired. The mean bias error (MBE), root mean square error (RMSE) and coefficient of determination (R^2) were also employed for statistical inference in this research.

3 Results and discussion

3.1 Comparison of ET_a Maps Derived from the Kc–NDVI and METRIC Methods

In this study, the METRIC model was implemented using the R-METRIC workflow in combination with the LandMOD ET Mapper (MATLAB environment) to estimate actual evapotranspiration (ET_a) and generate spatiotemporal ET_a fields constrained by local ground observations collected on satellite acquisition dates across the Akarsu Irrigation District (AID). The integration of local meteorological data into METRIC allowed for accurate representation of surface energy balance components, including net radiation (R_n), soil heat flux (G), and sensible heat flux (H), under the prevailing climatic and land surface conditions. For instance, Figure 4 illustrates that on 19 December 2019 (DOY 353), daily ET_a estimated by METRIC was 1.48 mm day⁻¹, whereas the K_c-NDVI method yielded a corresponding value of 0.72 mm day⁻¹. Similar discrepancies were observed at the beginning and end of the growing season, primarily when vegetation cover was sparse and NDVI values were low. Across all image acquisition dates, ET_a derived from the K_c-NDVI method was systematically evaluated against METRIC-based ET_a to assess the degree of agreement and quantify potential biases. This comparison provided a basis for evaluating the reliability and operational feasibility of the simplified K_c-NDVI approach in representing field-scale evapotranspiration dynamics.

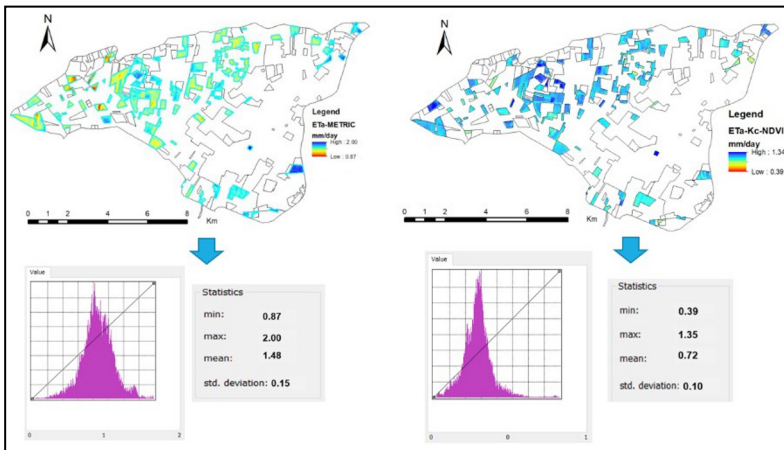
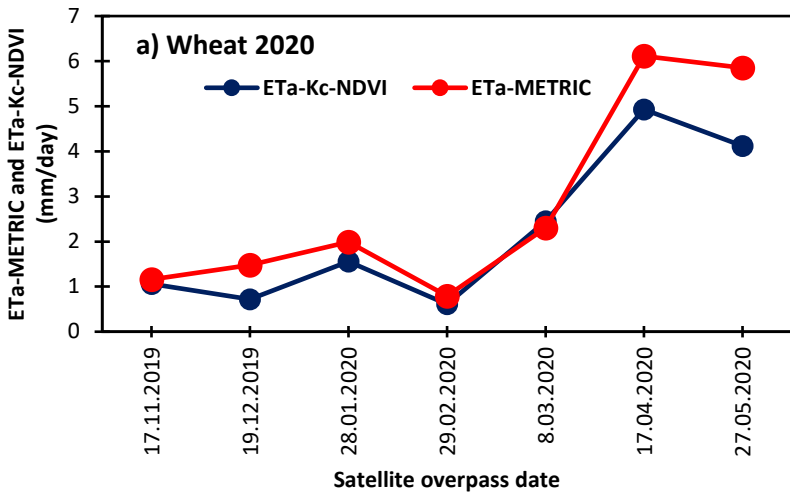


Fig. 4. Spatial distribution of wheat actual evapotranspiration (ET_a) estimated by the METRIC model (left) and the K_c-NDVI method (right) on DOY 353 (19 December 2019), expressed in millimeters per day (mm day⁻¹).

Figure 4 illustrates the spatial variability of wheat actual evapotranspiration (ET_a) derived from the METRIC and K_c-NDVI methods at the respective satellite overpass times. As summarized in Figure 5, ET_a estimated by METRIC was generally higher than that derived from the K_c-NDVI approach. This difference arises from the effective crop coefficient (K_c), expressed in METRIC as the reference evapotranspiration fraction (ET_rF), which tends to be greater than the K_c values obtained from NDVI-based

regressions. Because METRIC explicitly solves the full surface energy balance, it inherently integrates the effects of climatic, soil, and canopy factors on evapotranspiration, whereas the Kc–NDVI method relies primarily on empirical relationships between vegetation indices and crop coefficients. This observation aligns with previous findings that METRIC typically produces higher ET_a values than NDVI-based methods (e.g., Anderson et al., 2012; Reyes-González et al., 2018), largely because METRIC-derived Kc (ET_rF) represents the actual surface flux conditions more accurately than Kc values inferred from NDVI or standard tabulated coefficients (Allen et al., 1998).

Seasonal patterns were strongly stage-dependent. In both winters (2020 and 2021), METRIC- and Kc–NDVI-derived ET_a estimates converged during the mid-season period (Figures 4a and 4b), when the wheat canopy was dense and fully developed. In contrast, larger discrepancies were observed during early establishment and late senescence stages, when sparse or aging vegetation led to lower NDVI and, consequently, smaller NDVI-based Kc values. Meanwhile, METRIC-derived ET_a remained relatively higher due to its sensitivity to surface temperature and aerodynamic flux components that persist even under partial canopy cover.



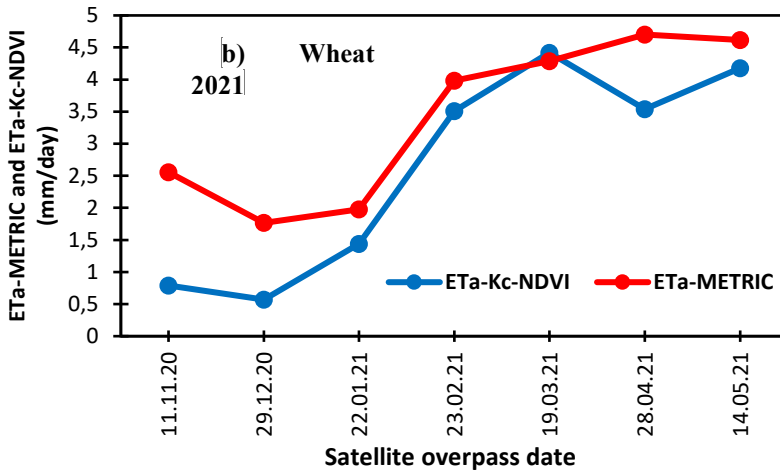


Fig. 5. Temporal variation of areal mean daily wheat actual evapotranspiration (ETA) estimated by the METRIC model and the Kc–NDVI method at satellite overpass times over the Akarsu Irrigation District (AID) during (a) 2020 and (b) 2021.

3.2 Linear Relationship and Statistical Agreement Between ETA–METRIC and ETA–Kc–NDVI

In this study, linear regression analysis was applied to assess the relationship between actual evapotranspiration (ETA) estimated by the METRIC model and the Kc–NDVI approach across the Akarsu Irrigation District (AID) (Figure 6). The scatterplot comparison demonstrated a strong agreement between the two methods for the 2020 and 2021 seasons, with Pearson correlation coefficients (r) of 0.98 and 0.94, respectively. The corresponding mean bias errors (MBE) were 0.61 and 0.78 mm day⁻¹ for 2020 and 2021, while the root mean square errors (RMSE) were 0.86 and 0.97 mm day⁻¹, respectively. These findings are consistent with earlier studies employing similar methodologies. For instance, the “golden-day” intercomparison reported close agreement between the Kc–NDVI and energy-balance models (METRIC/MSSEBS) over irrigated crops, with minimal biases under well-watered conditions (Trezza et al., 2006). Eddy-covariance validations have also shown that NDVI-derived basal crop coefficients (K_{cb}) reproduce seasonal ET patterns well during mid-season, though with reduced accuracy under sparse vegetation (Hunsaker et al., 2005; French et al., 2015). Furthermore, a multi-crop calibration over AmeriFlux sites revealed a robust linear Kc–NDVI relationship ($K_c = 1.457 \cdot NDVI - 0.1725$) with high fidelity (Kamble et al., 2013). Field-scale investigations have similarly reported strong Kc–NDVI performance ($R^2 \approx 0.77-0.86$) (Tagarakis et al., 2018), while basin-scale assessments mapping ETA from

NDVI-derived K_c have shown the highest agreement during mid-season, thereby supporting the operational use of NDVI-based parameterizations for regional water accounting (Babaeian et al., 2023). Our results also align with previous research conducted in the AID within the Lower Seyhan Plain, where METRIC-based ET_a exhibited good agreement with FAO-56 ET_c , and K_c derived from METRIC (ET_{rF}) correlated strongly with NDVI for summer crops (e.g., $r = 0.91$ for peanut; $r = 0.55$ for corn) (Alsenjar et al., 2023a). Similarly, an artificial neural network (ANN) framework combining MODIS NDVI and land surface temperature (LST) produced daily ET_a estimates with overall R^2 values ranging from 0.76 to 0.84, consistent with METRIC-derived ET_a (Karahan et al., 2024). Moreover, regional validation in nearby Adana demonstrated good agreement between pySEBAL-derived ET_a and lysimeter observations for soybean ($R^2 = 0.73$, $RMSE = 0.51 \text{ mm day}^{-1}$, $MBE = 0.04 \text{ mm day}^{-1}$) (Sawadogo et al., 2020). Additionally, crop-type mapping, ET_c estimates compiled for the AID were consistent with earlier direct-ET studies across the Cukurova region, emphasizing the transferability and reliability of coefficient-based evapotranspiration approaches in the Lower Seyhan Plain (Alsenjar et al., 2023b).

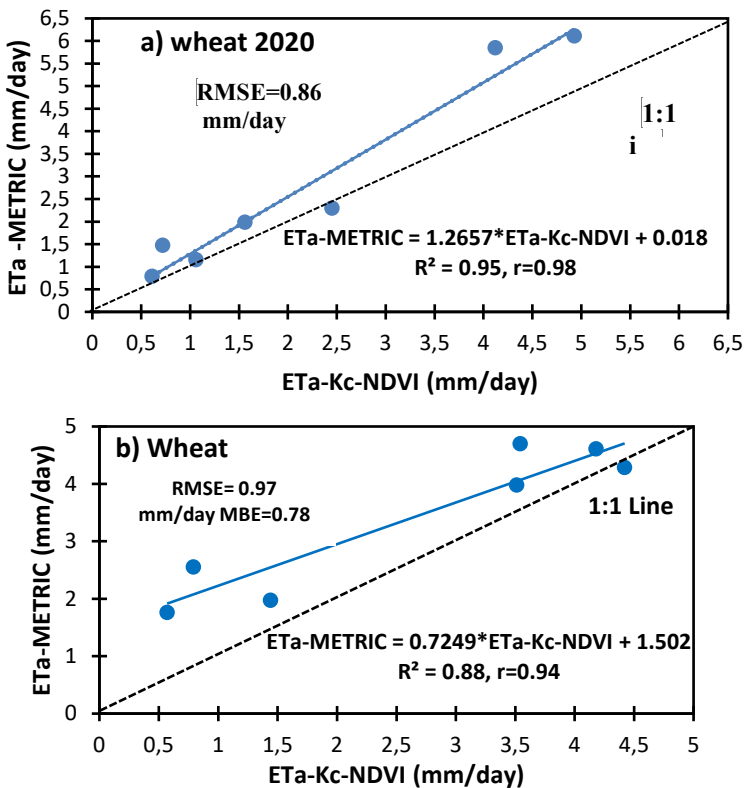


Fig. 6. Relationship between actual evapotranspiration (ET_a) estimated by the K_c -NDVI method and by the METRIC model for wheat during two growing seasons/years in the Akarsu Irrigation District, Türkiye.

This study addresses a key operational gap in the Lower Seyhan Plain by rigorously validating the *K_c-NDVI* approach, which uses an *NDVI-based* crop coefficient, against an independent energy-balance benchmark (*METRIC*) over two seasons and at the district level. Demonstrating robust agreement ($r = 0.98\text{--}0.94$; $\text{RMSE} = 0.86\text{--}0.97$ mm day⁻¹) and consistent performance with prior local and international studies shows that *K_c-NDVI* can deliver reliable, spatially explicit *ET_a* where flux towers or dense ground data are unavailable. Beyond confirming mid-season reliability, our results quantify the method's performance across winter conditions and mixed management, clarifying the conditions under which *K_c-NDVI* is most dependable. In practice, this allows for the reproducible, low-cost monitoring of ET for irrigation scheduling and water accounting in Mediterranean agro-ecosystems with limited data, thereby closing the evidence gap between plot-level demonstrations and scheme-level operations.

4 Conclusions and Recommendations

This study demonstrated that actual evapotranspiration (*ET_a*) estimated by the *METRIC* energy-balance model—based on comprehensive remote sensing (RS) inputs—closely aligns with *ET_a* derived from the simplified *K_c-NDVI* approach for irrigated wheat. To the best of our knowledge, this is the first study to produce high-resolution *ET_a* maps using both *METRIC* and *K_c-NDVI* methods in the intensively cultivated Akarsu Irrigation District (AID), which is prone to severe drought events, integrating local meteorological observations and multi-sensor satellite imagery for the 2020 and 2021 hydrological years. Consistent patterns were observed across both seasons: the *K_c-NDVI* method tended to underestimate *ET_a* relative to *METRIC* at the beginning and end of the winter season, when vegetation cover was sparse; however, it performed well during the mid-season when canopy development was at its peak. These findings indicate that the *K_c-NDVI* approach provides a reliable, low-data alternative for mid-season ET monitoring, while *METRIC* remains superior for capturing energy fluxes during early and late growth stages under partial canopy conditions. In practical terms, the dual-method framework offers scalable, field-level *ET_a* estimation at high spatial resolution and can be readily adapted to other irrigation schemes and climatic conditions. *ET_a* maps generated from both methods can directly support hydrological modeling, basin-scale water budgeting, and operational irrigation management—enabling more transparent water accounting and optimized allocation in data-limited regions.

Based on the findings and conclusions of this study, future research should focus on integrating the *K_c-NDVI* and *METRIC* frameworks with advanced data-driven techniques—such as *machine learning and data assimilation*—to establish an operational evapotranspiration monitoring system capable of supporting precision irrigation and adaptive irrigation water management under changing climate conditions.

Acknowledgements. The authors gratefully acknowledge the financial support provided by the Scientific Research Projects (BAP) Coordination Unit of Cukurova University under Project No. **FDK-2022-14907**.

Disclosure of Interests. The authors have no competing interests to declare that are relevant to the content of this article.

5 References

1. Allen, R.G, Tasumi, M., Morse, A., Trezza, R., Wright, J.L., Bastiaanssen, W.G.M., Kramber, W., Lorite, L., Robison, C.W. (2007a). Satellite-based energy balance for mapping evapotranspiration with internalized calibration, METRIC (applications). *J Irrig Drain Eng* 133:395 406.
2. Allen, R.G., Pereira, L.S., Raes, D., Smith. M. (1998). Crop evapotranspiration guidelines for computing crop water requirements, FAO Irrigation and Drainage Paper 56. FAO, Rome.
3. Allen. R.G., Tasumi, M., Trezza, R. (2007b). Satellite-based energy balance for mapping evapotranspiration with internalized calibration, METRIC (model). *J. Irrig. Drain. Eng.* 133:380 394.
4. Alsenjar, O., Çetin, M., Aksu, H., Gölpinar, M. S., & Akgül, M. A. (2023a). Actual evapotranspiration estimation using METRIC model and Landsat satellite images over an irrigated field in the Eastern Mediterranean Region of Turkey. *Mediterranean Geoscience Reviews*, 5, 35–49. <https://doi.org/10.1007/s42990-023-00099-y>
5. Alsenjar, O., Cetin, M., Aksu, H., Golpinar, M.S., Akgul M.A. (2023b). Actual evapotranspiration estimation using the METRIC model and Landsat satellite images over an irrigated field in the Eastern Mediterranean Region of Turkey. *Mediterranean Geoscience Reviews* (2023) 5:35–49 <https://doi.org/10.1007/s42990-023-00099-y>.
6. Anderson, M. C., Allen, R.G., Morse, A., Kustas, W. P. (2012). Use of Landsat thermal imagery in monitoring evapotranspiration and managing water resources. *Remote Sensing of Environment*, 122, 50-65. doi <http://dx.doi.org/10.1016/j.rse.2011.08.025>.
7. Babaeian, E., et al. (2023). Mapping vegetation-index-derived actual evapotranspiration across croplands in drylands using Google Earth Engine. *Remote Sensing*, 15(4), 1017. <https://doi.org/10.3390/rs15041017>
8. Bhattarai, N., Quackenbush, L.J., Im, J, Shaw, S. B, (2017). A new optimised algorithm for automating endmember pixel selection in the SEBAL and METRIC models. *Remote Sensing of Environment*, 196, 178-192. DOI: <https://doi.org/10.1016/j.rse.2017.05.009>.
9. Cetin M, Alsenjar O, Aksu H, Golpinar M. S, Akgul M. A (2023b). Estimation of crop water stress index and leaf area index based on remote sensing data, 2023. *Water Supply* 00:1. <https://doi.org/10.2166/ws.2023.051>.
10. Cetin M., 2020, "Agricultural Water Use. In Harmancioglu, N., Altinbilek, D. (Eds.), *Water Resources of Turkey: World Water Resources*", Vol. 2, Springer, Cham, 257-302.
11. Cetin, M., Alsenjar, O., Aksu, H., Golpinar, M.S., Akgul, M.A. (2023a). Comparing actual evapotranspiration estimations by METRIC to in-situ water balance measurements over an irrigated field in Turkey. *Hydrological Sciences Journal*, DOI: 10.1080/02626667.2023.

12. Cetin, M., Kaman, H., Kirda, C., Sesveren, S. (2020). Analysis of Irrigation Performance in Water Resources Planning and Management: A Case Study. *Fresenius Environmental Bulletin (FEB)*, vol 29. 05: 3409-3414.
13. El-shirbeny, M.A., Sciences, S., Ali, A. M., Sciences, S. (2015). Assessment of wheat crop coefficient using remote sensing techniques, (October), 10–16. <https://doi.org/10.13140/RG.2.1.1673.0325>.
14. Foolad, F., Blankenau, P., Kilic, A., Allen, R.G., Huntington, J.L., Erickson, T.A., Ozturk, D., Morton, C.G., Ortega, S., Ratcliffe, I., Franz, T.E, Thau, D, Moore, R., Gorelick, N., Kamble, B., Revelle, P., Trezza, R., Zhao, W., Robison, C.W.(2018). Comparison of the Automatically Calibrated Google Evapotranspiration Application-EEFlux and the Manually Calibrated METRIC Application. *Preprints* (2018), 2018070040. <https://doi.org/10.20944/preprints201807.0040.v1>.
15. French, A. N., Hunsaker, D. J., & Sanchez, C. A. (2015). Satellite-based NDVI crop coefficients and evapotranspiration with eddy covariance validation for durum wheat in the U.S. Southwest. *Agricultural Water Management*, 159, 123–138. <https://doi.org/10.1016/j.agwat.2015.06.001>
16. Hunsaker, D. J., Pinter, P. J., Jr., & Kimball, B. A. (2005). Wheat basal crop coefficients determined by normalized difference vegetation index. *Irrigation Science*, 24(1), 1–14. <https://doi.org/10.1007/s00271-005-0001-0>
17. Ibrkici, H., Cetin M., Karnez E., Flügel W. A., Tilkici B., Bulbul Y., Ryan J. (2015). Irrigation-induced nitrate losses assessed in a Mediterranean irrigation district. *Agric. Water Manage.*, 148, 223–231 (<http://dx.doi.org/10.1016/j.agwat.2014.10.007>).
18. Kamble, B., Kilic, A., & Hubbard, K. (2013). Estimating crop coefficients using remote sensing-based vegetation index. *Remote Sensing*, 5(4), 1588–1602. <https://doi.org/10.3390/rs5041588>
19. Karahan, H., Çetin, M., Can, M. E., & Alsenjar, O. (2024). Developing a new ANN model to estimate daily actual evapotranspiration using limited climatic data and remote sensing techniques for sustainable water management. *Sustainability*, 16(6), 2481. <https://doi.org/10.3390/su16062481>
20. Olmedo, G.F., Ortega-farias, S., Fonseca-luengo, D. (2016). Tools and functions to estimate actual evapotranspiration using land water: tools and functions to estimate actual evapotranspiration using land surface energy balance models. *The R Journal*, 8, 352. doi:10.32614/RJ-2016-051.
21. Rafn, E.B., Contor, B., Ames, D.P. (2009). Evaluation of a Method for Estimating Irrigated Crop-Evapotranspiration Coefficients from Remotely Sensed Data in Idaho, 134(6), 722–729. [https://doi.org/10.1061/\(ASCE\)0733-9437\(2008\)134](https://doi.org/10.1061/(ASCE)0733-9437(2008)134)
22. Reyes-Gonzalez, A., Hay, C., Kjaersgaard, J., & Neale, C. (2015). Use of Remote Sensing to Generate Crop Coefficient and Estimate Actual Crop Use of Remote Sensing to Generate Crop Coefficient and Estimate Actual Crop Evapotranspiration Introduction, (July). <https://doi.org/10.13031/aim.20152190105>.
23. Reyes-González, A., Kjaersgaard, J., Trooien, T., Hay, C., Ahiablame, L. (2018). Assessing accuracy of vegetation index method to estimate actual evapotranspiration. *Earth Sciences*. Vol. 7, No. 5, 2018, pp. 227-235. doi: 10.11648/j.earth.20180705.14.
24. Rouse, J.W., Haas, R.H., Schell, J.A., Deering, D.W. (1973). Monitoring Vegetation Systems in the Great Plains with ERTS. In *Proceedings of Third ERTS Symposium*, Washington, DC, USA, 10–14 December 1973; Volume 1, pp. 309–317.

25. Sawadogo, A., Hessels, T., Gündoğdu, K. S., Demir, A. O., Ünlü, M., & Zwart, S. J. (2020). Comparative analysis of the pySEBAL model and lysimeter for estimating actual evapotranspiration of soybean crop in Adana, Turkey. *International Journal of Engineering and Geosciences*, 5(2), 60–65. <https://doi.org/10.26833/ijeg.573503>
26. Su, Z. (2002). The surface energy balance system (SEBS) for estimation of turbulent heat fluxes. *Hydrol Earth Syst Sci* 6:85 100.
27. Tagarakis, A. C., et al. (2018). A refined method for rapidly determining the crop coefficient using NDVI. *Computers and Electronics in Agriculture*, 149, 1–9. <https://doi.org/10.1016/j.compag.2017.10.028>
28. TAGEM-DSI. (2017). Plant water consumption of irrigated plants in Türkiye. Ankara, Türkiye: The Republic of Türkiye, Ministry of Agriculture and Forestry, General Directorates of Agricultural Research and Policies (TAGEM) and State Hydraulic Works (DSI), Published by TAGEM. 590. (In Turkish).
29. Trezza, R., Allen, R. G., & Tasumi, M. (2006). Golden-day comparison of methods to retrieve ET (Kc–NDVI, Kc-analytical, MSSEBS, METRIC). *AIP Conference Proceedings*, 852, 193–201. <https://doi.org/10.1063/1.2349362>
30. Zhang, X.C., Wu, J.W., Wu, H.Y., Li, Y. (2011). Simplified SEBAL method for estimating vast areal evapotranspiration with MODIS data. *WaterSci Eng* 4:24 35. <https://doi.org/10.3882/j.1674-2370,2011.01.003>.

Open Access This chapter is licensed under the terms of the Creative Commons Attribution-NonCommercial 4.0 International License (<http://creativecommons.org/licenses/by-nc/4.0/>), which permits any noncommercial use, sharing, adaptation, distribution and reproduction in any medium or format, as long as you give appropriate credit to the original author(s) and the source, provide a link to the Creative Commons license and indicate if changes were made.

The images or other third party material in this chapter are included in the chapter's Creative Commons license, unless indicated otherwise in a credit line to the material. If material is not included in the chapter's Creative Commons license and your intended use is not permitted by statutory regulation or exceeds the permitted use, you will need to obtain permission directly from the copyright holder.

